Hadron Collider Physics Symposium (HCP2008), Galena, Illinois, USA

Search for the Wh Production Using High-p_T Isolated Like-Sign Dilepton Events in Run-II with 1.9 fb^{-1}

Toru Okusawa, Yoshihiro Seiya, Takayuki Wakisaka and Kazuhiro Yamamoto
Osaka City University, Japan, on behalf of the CDF Collaboration

We search for the neutral higgs production associated with the W boson using high-p_T isolated like-sign dilepton events in $p\bar{p}$ collisions at $\sqrt{s} = 1.96$ TeV. The data were collected with the CDF-II detector at the Fermilab Tevatron collider and correspond to an integrated luminosity of 1.9 fb^{-1}. We examine the dilepton events on the plane of the 2nd lepton p_T (p_{T2}) versus the p_T of dilepton system (p_{T12}) and tune the final cut to maximize the sensitivity on the plane. We set the final cut to the 2nd lepton p_T greater than 20 GeV/c and the p_T of dilepton system greater than 15 GeV/c. The expected number of signal events is 0.46 for the fermiophobic higgs of the mass 110 GeV/c^2 and 0.19 for the mass 160 GeV/c^2 assuming the Standard Model cross section. The number of events for the Standard Model higgs is 0.02 and 0.18 for 110 GeV/c^2 and 160 GeV/c^2, respectively. The expected number of backgrounds is 3.23 $\pm$ 0.69, while we observed 3 events in the data. From these results, we obtain the limits on $\sigma(p\bar{p} \to Wh) \times Br(h \to W^+W^-)$ of 2.2 pb for the higgs of 110 GeV/c^2 and 1.4 pb for 160 GeV/c^2 at the 95% confidence level.

1. Introduction

In the Standard Model, the higgs boson is introduced to explain the electroweak symmetry breaking and the origin of fermion masses. The direct search at the CERN e^+e^- collider (LEP2) presents a lower limit on the higgs boson mass of $m_h > 114.4$ GeV/c^2 at the 95% confidence level (C.L.). Indirect measurements, electroweak global fits, give an upper limit of 144 GeV/c^2 at the 95% C.L. which increases to 182 GeV/c^2 when the direct search is included [1].

Our physics objective is to search for the low-mass fermiophobic higgs and the high-mass Standard Model higgs boson using like-sign dilepton events produced by

$$qq' \to W^{\pm}h \to W^{\pm}W^*W^* \to \ell^{\pm}\ell^{\pm} + X.$$

The relevant higgs mass regions are above 110 GeV/c^2 for the fermiophobic higgs where the branching fraction of $h \to W^*W^*$ supersedes that of $h \to \gamma\gamma$, and above 160 GeV/c^2 for the Standard Model higgs where the branching fraction of $h \to b\bar{b}$ is overtaken by this channel.

The fermiophobic higgs boson has no coupling to the fermions. Existence of the fermiophobic higgs could be an indication that the origin of particle masses would be different for the bosons and the fermions. Such a particle can also arise as a CP-even scalar h^0 in the two higgs doublet model (2HDM) type I. The model has seven degrees of freedom: the five particle masses (h^0,H^0, A^0, $H^{\pm}$) and two angles (α, β). In the type I, the lightest CP-even scalar h^0 couples to a fermion proportionally to $\cos\alpha$, and the h^0 becomes a fermiophobic higgs when $\alpha = \pi/2$.

2. Data Sample & Event Selection

This analysis is based on the data with an integrated luminosity of 1.9 fb^{-1} collected with the CDF-II detector between March 2002 and May 2007. Detailed descriptions of the CDF-II detector can be found in [3]. The data are collected with inclusive lepton triggers that requires an electron with transverse energy (E_T) > 18 GeV or a muon with transverse momentum (p_T) > 18 GeV/c. Starting from the inclusive lepton datasets, we apply a number of event selection criteria to obtain a baseline dilepton sample. The events are required to have primary vertices within the region to ensure well-defined measurement of collisions by the detector and to pass a cosmic-ray veto. We select events at least one electron with $E_T > 20$ GeV and $p_T > 10$ GeV/c, or muon with $p_T > 20$ GeV/c, which

is considered to be responsible for firing the triggers we have chosen, and at least one other electron with $E_T >$ 6 GeV and $p_T > 6$ GeV/c, or muon with $p_T > 6$ GeV/c, as the baseline dilepton selection. The leptons must be found in the central detector ($|\eta| < 1.1$) and within fiducial regions of the sub-detectors. They are also required to be isolated in terms of the calorimeter cone-isolation, with a cone size of $R = 0.4$, to be less than 2 GeV, where $R = \sqrt{(\Delta\eta)^2 + (\Delta\phi)^2}$ is the radius in the η-ϕ space, $\eta = -\ln(\tan\theta/2)$ is the pseudorapidity, the θ is the polar angle with respect to the proton beam direction, and ϕ is the azimuthal angle. The leptons must have a well-measured track, found both in the outer tracking chamber and the inner silicon detector, with the z coordinate and the impact parameter at the closest approach point to the beamline being consistent with coming from the primary vertex. We then apply a series of lepton identification cuts which impose various internal consistencies of information obtained from sub-detectors and require detector responses consistent with electrons or muons. If the electron is consistent with being due to a photon conversion as indicated by the presence of an additional nearby track, the electron is vetoed.

For the exactly two-lepton events passing our selection above, we explicitly require a cut to ensure that the two leptons are coming from the same vertex, and also apply a dilepton mass cut ($M_{\ell\ell} > 12$ GeV/c^2) and a Z-event veto. We finally require the like-sign charge combination to complete the baseline event selection. The final cut to obtain the result is discussed in §4.

3. Backgrounds

Although the like-sign requirement is quite effective to suppress QCD and known electroweak processes, we expect that fake-lepton backgrounds and residual photon-conversions still remain at a considerable level in the events of our signature. They are estimated by data-driven methods, while other backgrounds containing prompt real-leptons (physics backgrounds) are estimated by Monte Carlo (MC) data.

3.1. Physics Backgrounds

The physics backgrounds can be classified into reducible and irreducible backgrounds. The reducible backgrounds are Drell-Yan, WW, $t\bar{t}$, and W + (heavy-flavor hadrons), while irreducible backgrounds are WZ and WW. The reducible backgrounds are reduced by the isolation cut and like-sign requirement. Contributions of the irreducible backgrounds are small due to their small production cross sections, which are further suppressed by the Z-event veto. Since fake-leptons and residual photon-conversions are estimated separately using real data, we reject them found in the MC by looking at the generator-level information to avoid double counting.

3.2. Residual Photon-Conversion Background

The residual photon-conversion backgrounds arise from an electron originating from the photon conversion with an unobserved partner track due to its low momentum. We estimate the backgrounds by multiplying lepton + conversion events by residual photon-conversion rate ($R_{\rm res}$). We define the rate by

$$R_{\rm res} = \frac{1 - \varepsilon_{\rm con}}{\varepsilon_{\rm con}},$$

where $\varepsilon_{\rm con}$ is the conversion detection efficiency. The efficiency is measured by comparing the conversions found in the real data with conversion MC samples that are tuned to match with the sub-sample of real conversions in the high-p_T region of partner-tracks where the efficiency is well known. The residual conversion rate is parametrized by the parent photon p_T and is shown in FIG. 1 left.

3.3. Fake Lepton Background

The fake electron backgrounds are interactive $\pi^{\pm}$, overlap of π^0 and a track, and residual photon-conversions. The fake muon backgrounds are punch-through hadrons and decay-in-flight muons from $\pi^{\pm}$ and $K^{\pm}$. We also regard leptons from semileptonic decays of heavy-flavor hadron as one of fake lepton backgrounds. These background objects are common in generic QCD events. We estimate the backgrounds by multiplying lepton + isolated track events by the fake lepton rates derived from inclusive jet samples. The fake lepton rate ($R_{\rm fake}$) is defined as a rate of leptons in the jet samples relative to isolated tracks with certain energy depositions especially in the hadron calorimeters. The p_T cut is 6 GeV/c in accordance with the lower p_T cut of our baseline event selection. We reject W and Z events to find leptons in the jet samples to avoid prompt real-leptons from electroweak processes. The fake lepton rate is shown in FIG. 1 right. The fake electron rates go through corrections to subtract residual conversions in the jet samples because we estimate the amount of residual photon-conversion events separately as mentioned in the previous section.

4. Final Cut

Comparisons of kinematics distributions and the number of events between the data and the background prediction for the like-sign dilepton events after the baseline selection are shown in FIG. 2 and TABLE I, where we categorize electron-muon pairs into $e\mu$ and μe depending on which lepton has the leading p_T and fires the corresponding lepton trigger.

We further examine the baseline like-sign dilepton events on the 2 dimensional plane of the 2nd lepton p_T (p_{T2}) versus the dilepton system p_T (p_{T12}). By scanning this 2D plane with moving p_{T2} and p_{T12} cut values, we see no significant discrepancies between the data and the background expectations. We then determine the optimized cut values for signal events to get minimized expected upper limit on the production cross section times branching fraction (FIG. 3). The final cut is set to $p_{T2} \geq 20$ GeV/c and $p_{T12} \geq 15$ GeV/c. With this cut, we define 4 regions:

- region1 : $p_{T2} \geq 20$ GeV/c and $p_{T12} < 15$ GeV/c
- region2 : $p_{T2} < 20$ GeV/c and $p_{T12} < 15$ GeV/c
- region3 : $p_{T2} < 20$ GeV/c and $p_{T12} \geq 15$ GeV/c
- region4 : $p_{T2} \geq 20$ GeV/c and $p_{T12} \geq 15$ GeV/c

TABLE II shows event counting for each region. We see reasonable agreement between the expected number of backgrounds and observed events.

5. Efficiency of Signal and Systematic Uncertainties

TABLE III (left) shows the signal efficiencies, where the denominator is the number of $W^{\pm}h \rightarrow W^{\pm}W^*W^* \rightarrow$ at least 2-lepton events. The branching fraction corresponding to events with at least 2 leptons from triple Ws is about 0.12. The efficiencies are multiplied with MC scale factors which are obtained by using Drell-Yan events found in the data and MC. The uncertainties in TABLE III (right) include MC statistics and uncertainties of MC scale factors. We estimate systematic uncertainties from several other sources for the signal efficiencies as summarized in TABLE III (right).

Systematic uncertainties for the background estimation are already included in TABLES I and II, which include uncertainties of residual photon-conversion estimation, fake-lepton estimation, and MC scale factors for the MC-based background estimations.

6. Results

We find the expected number of backgrounds is 3.23 ± 0.69 events, while we observed 3 events in the data. From these results, we set the 95% C.L. upper limits on the cross section times branching fraction $\sigma(p\bar{p} \to Wh) \times Br(h \to W^+W^-)$ with the Bayesian approach as 2.2 pb for the higgs of the mass 110 GeV/c^2 and 1.4 pb for 160 GeV/c^2. TABLE IV shows the limit for each higgs mass point from 110 GeV/c^2 to 200 GeV/c^2. We also obtain the ratios of the limit to the Standard Model cross sections and to the fermiophobic higgs cross sections (assuming the Standard Model production cross sections) with taking into account of uncertainties of these theoretical predictions in the limit calculations, which are shown in TABLE V.

7. Conclusions

We searched for the neutral higgs production associated with the W boson using high-p_T like-sign dilepton events with the data corresponding to an integrated luminosity of 1.9 fb^{-1}. We did not see any significant disagreements between background expectations and the data. Given this, we tuned the final cut on the 2nd lepton p_T and the p_T of dilepton system in order to obtain the limit-best result. We found that the 2nd lepton p_T cut of 20 GeV/c and the dilepton-system p_T cut of 15 GeV/c was a reasonable choice. With this final cut, we obtained the expected number of fermiophobic higgs events for the mass 110 GeV/c^2 to be 0.46 assuming the Standard Model production cross section and 0.19 for the 160 GeV/c^2 higgs. The expected number of backgrounds in the final sample was 3.23 ± 0.69, while the actual number of observed events was 3. We obtained the upper limits on the production cross-section times the branching fraction for the higgs with masses in the region from 110 GeV/c^2 to 200 GeV/c^2, 2.2 pb for the 110 GeV/c^2 higgs and 1.4 pb for 160 GeV/c^2.

Acknowledgments

We thank the Fermilab staff and the technical staffs of the participating institutions for their vital contributions. This work was supported by the U.S. Department of Energy and National Science Foundation; the Italian Istituto Nazionale di Fisica Nucleare; the Ministry of Education, Culture, Sports, Science and Technology of Japan; the Natural Sciences and Engineering Research Council of Canada; the National Science Council of the Republic of China; the Swiss National Science Foundation; the A.P. Sloan Foundation; the Bundesministerium fuer Bildung und Forschung, Germany; the Korean Science and Engineering Foundation and the Korean Research Foundation; the Particle Physics and Astronomy Research Council and the Royal Society, UK; the Russian Foundation for Basic Research; the Comision Interministerial de Ciencia y Tecnologia, Spain; and in part by the European Community's Human Potential Programme under contract HPRN-CT-20002, Probe for New Physics.

Table I: Background expectation and observed number of events for the like-sign dilepton events for each dilepton channel before the final cut.

	ee	$e\mu$	μe	$\mu\mu$	Total
Fakes	46.1	29.8	30.4	19.8	126.1
Photon-conversions	6.2	-0.4	6.4	—	12.2
Total	52.3 ± 6.9	29.4 ± 4.0	36.8 ± 5.1	19.7 ± 3.1	138.3 ± 9.2
(Stat.)	± 2.2	± 1.2	± 1.7	± 0.8	± 3.1
(Syst.)	± 6.2	± 3.8	± 4.8	± 3.0	± 8.7
$W \to e\nu/\mu\nu$	0.00	0.00	0.00	0.00	0.00
$Z/\gamma^* \to ee/\mu\mu$	0.00	0.00	0.09	0.09	0.18
$Z/\gamma^* \to \tau\tau$	0.00	0.00	0.00	0.00	0.00
$t\bar{t}$	0.00	0.01	0.00	0.00	0.01
Diboson	0.46	0.65	0.79	0.82	2.58
Total MC	0.46 ± 0.03	0.66 ± 0.06	0.88 ± 0.11	0.91 ± 0.11	2.86 ± 0.37
(Stat.)	± 0.01	± 0.02	± 0.09	± 0.09	± 0.13
(Syst.)	± 0.03	± 0.03	± 0.05	± 0.04	± 0.07
(Luminosity)	± 0.03	± 0.04	± 0.05	± 0.05	± 0.17
Fermiophobic higgs	0.227 ± 0.013	0.224 ± 0.013	0.271 ± 0.016	0.214 ± 0.012	0.938 ± 0.050
(110 GeV/c^2)					
(Stat.)	± 0.004	± 0.004	± 0.004	± 0.004	± 0.009
(Syst.)	± 0.003	± 0.002	± 0.002	± 0.004	± 0.014
(Luminosity)	± 0.013	± 0.013	± 0.016	± 0.012	± 0.050
SM higgs	0.063 ± 0.003	0.061 ± 0.003	0.084 ± 0.005	0.064 ± 0.003	0.272 ± 0.016
(160 GeV/c^2)					
(Stat.)	± 0.001	± 0.001	± 0.001	± 0.001	± 0.002
(Syst.)	± 0.001	± 0.001	± 0.001	± 0.001	± 0.003
(Luminosity)	± 0.003	± 0.003	± 0.005	± 0.003	± 0.016
Total expected	52.8 ± 6.6	30.6 ± 4.0	37.6 ± 5.1	20.7 ± 3.1	141.7 ± 9.2
Data	51	26	41	16	134

Table II: Background expectation and observed number of events for the like-sign dilepton events for each region as defined in the texts. The region 4 correspods to the signal region after the final cut.

	Regions				
	1	2	3	4	Total
Fakes	0.47	27.8	96.5	1.14	125.9
Photon-conversions	0.52	0.5	10.5	0.70	12.2
Total	0.99 ± 0.35	28.3 ± 2.1	107.0 ± 5.1	1.84 ± 0.68	138.1 ± 6.1
(Stat.)	± 0.23	± 1.8	± 3.6	± 0.30	± 4.1
(Syst.)	± 0.27	± 1.1	± 3.6	± 0.61	± 4.5
$W \to e\nu/\mu\nu$	0.00	0.00	0.00	0.00	0.00
$Z/\gamma^* \to ee/\mu\mu$	0.00	0.12	0.12	0.00	0.23
$Z/\gamma^* \to \tau\tau$	0.00	0.00	0.00	0.00	0.00
$t\bar{t}$	0.00	0.00	0.00	0.01	0.01
Diboson	0.11	0.06	1.05	1.38	2.60
Total MC	0.11 ± 0.01	0.17 ± 0.12	1.16 ± 0.14	1.40 ± 0.09	2.84 ± 0.24
(Stat.)	± 0.01	± 0.12	± 0.12	± 0.02	± 0.17
(Syst.)	± 0.00	± 0.00	± 0.01	± 0.01	± 0.02
(Luminosity)	± 0.01	± 0.01	± 0.07	± 0.08	± 0.17
Fermiophobic higgs (110 GeV/c^2)	0.036 ± 0.002	0.014 ± 0.003	0.418 ± 0.026	0.464 ± 0.029	0.932 ± 0.058
(Stat.)	± 0.001	± 0.001	± 0.006	± 0.006	± 0.009
(Syst.)	± 0.000	± 0.002	± 0.006	± 0.006	± 0.014
(Luminosity)	± 0.002	± 0.001	± 0.025	± 0.028	± 0.056
SM higgs (160 GeV/c^2)	0.011 ± 0.001	0.002 ± 0.000	0.075 ± 0.004	0.183 ± 0.011	0.272 ± 0.016
(Stat.)	± 0.000	± 0.000	± 0.001	± 0.002	± 0.002
(Syst.)	± 0.000	± 0.000	± 0.001	± 0.002	± 0.003
(Luminosity)	± 0.001	± 0.000	± 0.004	± 0.011	± 0.016
Total expected	1.10 ± 0.35	28.5 ± 2.1	108.1 ± 5.1	3.23 ± 0.69	141.0 ± 6.1
Data	2	23	106	3	134

Table III: Efficiencies for higgs events shown step by step for each higgs mass (left) and Systematic uncertainties of the signal efficiency (right).

Mass (GeV/c^2)	Lepton ID (%)	Dilepton cuts (%)	Like-sign (%)	Z veto (%)	Final cut (%)
110	6.98 ± 0.10	6.77 ± 0.09	2.29 ± 0.03	2.11 ± 0.03	1.05 ± 0.01
120	7.41 ± 0.10	7.23 ± 0.10	2.43 ± 0.03	2.23 ± 0.03	1.16 ± 0.02
130	7.81 ± 0.11	7.66 ± 0.10	2.54 ± 0.04	2.33 ± 0.03	1.33 ± 0.02
140	8.26 ± 0.11	8.11 ± 0.11	2.68 ± 0.04	2.45 ± 0.03	1.48 ± 0.02
150	8.48 ± 0.11	8.35 ± 0.11	2.71 ± 0.04	2.45 ± 0.03	1.57 ± 0.02
160	8.41 ± 0.11	8.29 ± 0.11	2.63 ± 0.04	2.36 ± 0.03	1.59 ± 0.02
170	8.58 ± 0.11	8.46 ± 0.11	2.70 ± 0.04	2.43 ± 0.03	1.67 ± 0.02
180	9.08 ± 0.11	8.98 ± 0.11	2.85 ± 0.04	2.53 ± 0.03	1.79 ± 0.02
190	9.55 ± 0.12	9.46 ± 0.12	3.12 ± 0.04	2.76 ± 0.04	1.98 ± 0.03
200	9.76 ± 0.12	9.68 ± 0.12	3.25 ± 0.04	2.87 ± 0.04	2.10 ± 0.03

Source	Uncertainty				
	ee (%)	$e\mu$ (%)	μe (%)	$\mu\mu$ (%)	$\ell\ell$ (%)
Monte-Carlo statistics	2.6	2.4	2.1	2.2	1.6
Monte-Carlo scale factors	1.1	1.0	1.3	1.2	1.2
Parton distribution function	1.9	1.8	2.1	2.0	1.9
Initial state radiation	5.1	5.2	7.4	2.5	4.0
Final state radiation	5.2	6.8	7.5	3.7	4.1
Z Cross Section	3.4	3.4	3.4	3.4	3.4
Luminosity	6.0	6.0	6.0	6.0	6.0
Total	10.7	11.7	13.1	9.0	9.6

Table IV: Cross section upper limit at the 95% confidence level.

Mass (GeV/c^2)	Expected Median (pb)	Expected Mean (pb)	Observed (pb)
110	$2.2^{+0.4}_{-0.7}$	2.4 ± 0.8	2.2
120	$2.0^{+0.4}_{-0.7}$	2.2 ± 0.8	2.0
130	$1.8^{+0.3}_{-0.6}$	1.9 ± 0.7	1.8
140	$1.6^{+0.3}_{-0.5}$	1.7 ± 0.6	1.6
150	$1.5^{+0.3}_{-0.5}$	1.6 ± 0.6	1.5
160	$1.5^{+0.3}_{-0.5}$	1.6 ± 0.5	1.5
170	$1.4^{+0.3}_{-0.5}$	1.5 ± 0.5	1.4
180	$1.3^{+0.3}_{-0.4}$	1.4 ± 0.5	1.3
190	$1.2^{+0.2}_{-0.4}$	1.3 ± 0.4	1.2
200	$1.1^{+0.2}_{-0.4}$	1.2 ± 0.4	1.1

Table V: Ratio of the cross section upper limit to the Standard Model prediction (left) and to the fermiophobic higgs.

Mass (GeV/c^2)	Expected Median	Expected Mean	Observed
110	$281.8^{+57.1}_{-92.9}$	305.7 ± 111.2	281.8
120	$115.7^{+23.4}_{-38.1}$	125.5 ± 45.6	115.7
130	$60.2^{+12.2}_{-19.8}$	65.3 ± 23.7	60.2
140	$40.8^{+8.2}_{-13.4}$	44.3 ± 16.1	40.8
150	$34.9^{+7.0}_{-11.5}$	37.8 ± 13.7	34.9
160	$33.1^{+6.3}_{-10.9}$	35.9 ± 13.0	33.1
170	$38.3^{+7.7}_{-12.6}$	41.5 ± 15.1	38.3
180	$47.2^{+9.5}_{-15.5}$	51.2 ± 18.6	47.2
190	$54.1^{+10.9}_{-17.8}$	58.7 ± 21.3	54.1
200	$64.2^{+13.0}_{-21.1}$	69.6 ± 25.3	64.2

Mass (GeV/c^2)	Expected Median	Expected Mean	Observed
110	$12.9^{+2.6}_{-4.2}$	14.0 ± 5.1	12.9
120	$15.7^{+3.2}_{-5.2}$	17.1 ± 6.2	15.7
130	$18.4^{+4.3}_{-6.0}$	20.0 ± 7.2	18.4
140	$21.5^{+5.3}_{-7.1}$	23.4 ± 8.5	21.5
150	$26.3^{+6.3}_{-8.6}$	28.6 ± 10.4	26.3
160	$31.4^{+6.5}_{-10.3}$	34.0 ± 12.4	31.4
170	$37.9^{+7.7}_{-12.4}$	41.1 ± 14.9	37.9
180	$47.2^{+9.5}_{-15.5}$	51.2 ± 18.6	47.2
190	$54.1^{+10.9}_{-17.8}$	58.7 ± 21.3	54.1
200	$64.2^{+13.0}_{-21.1}$	69.6 ± 25.3	64.2

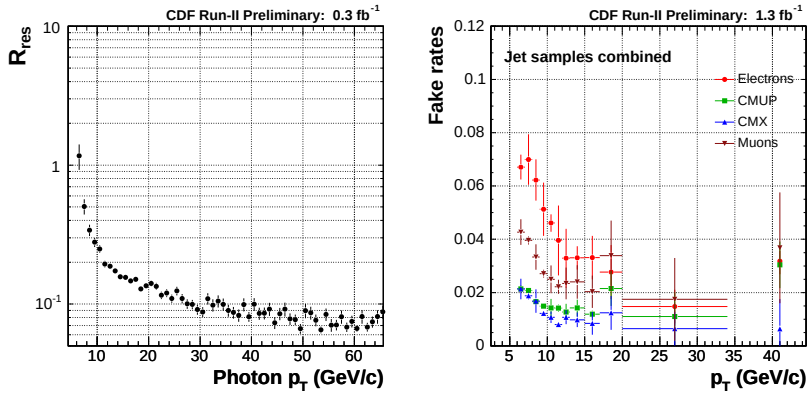

Figure 1: Residual photon-conversion rates as a function of photon p_T (left) and Fake-lepton rates as a function of isolated track p_T for each lepton object(right).

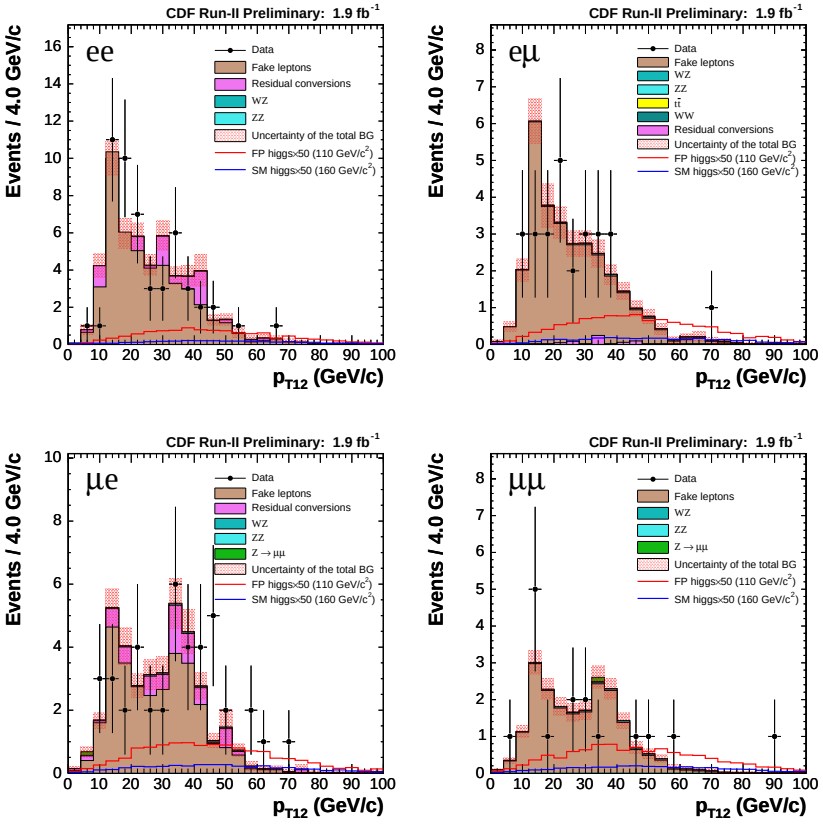

Figure 2: Comparison of kinematic distributions (dilepton system p_T) between the data and the background prediction for the like-sign dilepton events.

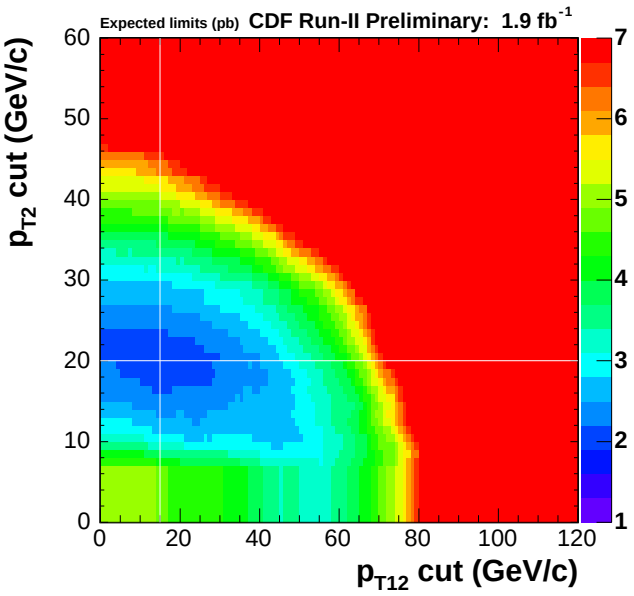

Figure 3: Expected upper limit on the $\sigma(Wh) \times Br(h \to W^+W^-)$ at the 95% confidence level on the 2 dimensional plane.

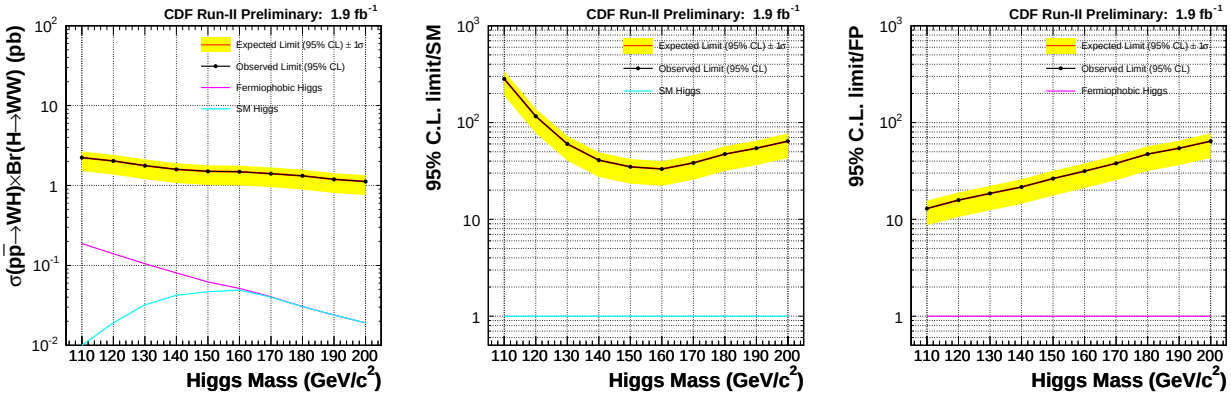

Figure 4: Cross section upper limit at the 95% confidence level (left) and Ratio of cross section upper limit to the prediction of the Standard Model (center) and fermiophobic higgs (right).

References

[1] LEP Electroweak Working Group, http://lepwwg.web.cern.ch/LEPEWWG/.

[2] A. Stange, W. Maricano, and S. Willenbrock, Phys. Rev. D **49**, 1354 (1994).

[3] F. Abe, et al., Nucl. Instrum. Methods Phys. Res. A **271**, 387 (1988); D. Amidei, et al., Nucl. Instum. Methods Phys. Res. A **350**, 73 (1994); F. Abe, et al., Phys. Rev. D **52**, 4784 (1995); P. Azzi, et al., Nucl. Instrum. Methods Phys. Res. A **360**, 137 (1995); The CDFII Detector Technical Design Report, Fermilab-Pub-96/390-E